Synthesis of Fractional-order PI Controllers and Fractional-order Filters for Industrial Electrical Drives

Paolo Lino, *Member, IEEE,* Guido Maione, *Senior Member, IEEE,* Silvio Stasi, Fabrizio Padula, and Antonio Visioli, *Senior Member, IEEE*

***Abstract*—This paper introduces an electrical drives control architecture combining a fractional-order controller and a set-point pre-filter. The former is based on a fractional-order proportional-integral (PI) unit, with a non-integer order integral action, while the latter can be of integer or non-integer type. To satisfy robustness and dynamic performance specifications, the feedback controller is designed by a loop-shaping technique in the frequency domain. In particular, optimality of the feedback system is pursued to achieve input-output tracking. The set-point pre-filter is designed by a dynamic inversion technique minimizing the difference between the ideal synthesized command signal (i.e., a smooth monotonic response) and the pre-filter step response. Experimental tests validate the methodology and compare the performance of the proposed architecture with well-established control schemes that employ the classical PI-based symmetrical optimum method with a smoothing pre-filter.**

***Index Terms*—Dynamic inversion, electrical drives, fractional-order PI controller, loop-shaping, set-point pre-filter.**

I. Introduction

In the last two decades, the applications of fractional calculus spread across several engineering fields [1], [2], ranging from control systems [3], [4] to electrical circuits [5], to signal processing and communications [6]−[8], to antennas and propagation [9], [10], etc. In particular, several efforts aimed to take advantage of fractional differentiation/integration for developing effective and easy-to-use control design methods and tuning techniques [11]. Frequently, the innovations are based on the idea of extending the proportional-integral-derivative (PID) controllers by differential or integral operators of non-integer order [12].

Manuscript received November 3, 2015; accepted April 1, 2016. Fabrizio Padula's research contributing to these results has been partially supported by the Australian Research Council (DP160104994). Recommended by Associate Editor Dingyü Xue.

Citation: P. Lino, G. Maione, S. Stasi, F. Padula, and A. Visioli, "Synthesis of fractional-order PI controllers and fractional-order filters for industrial electrical drives," *IEEE/CAA Journal of Automatica Sinica*, vol. 4, no. 1, pp. 58−69, Jan. 2017.

P. Lino, G. Maione, and S. Stasi are with the Dipartimento di Ingegneria Elettrica e dell'Informazione, Politecnico di Bari, Bari I-70125, Italy (e-mail: paolo.lino@poliba.it; guido.maione@poliba.it; silvio.stasi@poliba.it).

F. Padula is with the Department of Mathematics and Statistics, Curtin University, Perth WA6102, Australia (e-mail: fabrizio.padula@curtin.edu.au).

A. Visioli is with the Department of Mechanical and Industrial Engineering, University of Brescia, Brescia 25123, Italy (e-mail: antonio.visioli@unibs.it).

Color versions of one or more of the figures in this paper are available online at http://ieeexplore.ieee.org.

Digital Object Identifier 10.1109/JAS.2017.7510325

These controllers are often named fractional-order controllers (FOC), where the order of differentiation and integration can be any non-integer number, even complex [13]. However, to be successful in industrial applications, the FOC must compete with the wide diffusion of PID controllers [14]. Namely, it is well-known that FOC may guarantee superior robustness and dynamic performance indexes with respect to PID, especially if the controlled plants are themselves modeled as fractional-order systems [15]. However, affordable realizations are required for low-cost implementation. To this aim, the irrational transfer functions of FOC must be approximated by rational transfer functions. Then, efficient, easy-to-use, and convenient realization techniques are necessary. Indeed a good trade-off between accuracy and efficiency would be a great benefit for many industrial control loops using PID [14].

Regarding robust control systems, the seminal Bode's idea is to approximate an ideal loop gain ω_c/s^ν as much as possible. This transfer function includes an integrator of non-integer (fractional) order ν and the gain crossover angular frequency ω_c [11], [12], [16], [17]. The solutions based on integration of non-integer order reduce the sensitivity of the control loop to gain variations and to parametric uncertainties and achieve a better disturbance rejection. However, to be more accepted in industry, the FOC must easily achieve good time- or frequency-domain performance specifications and improve the robustness guaranteed by PID-based solutions. On the other hand, to obtain the same robustness of FOC, often more complex high integer-order controllers are necessary.

Hence this paper analyzes the benefits and limits of a new scheme with fractional-order PI (FOPI) controllers and fractional-order filters. The control scheme is tested on real electrical drives, that are important constituent parts of many industrial control systems. There are many approaches to design and then realize FOC (e.g., see [11], [12], [17]−[20]). In this paper, a new methodology is proposed to combine: 1) a loop-shaping strategy to design a feedback FOPI controller and 2) an input-output inversion technique to design an integer or non-integer order set-point pre-filter. The main contributions are the following ones:

1) extending the symmetrical optimum tuning method for classical PI to the FOPI counterparts, i.e., extending a well-known and widely used method to FOPI to make easier the acceptance from the industrial drives area;

2) extending, in this context, the standard combination of

the PI with a smoothing pre-filter to the combination of the FOPI with an integer- or fractional-order pre-filter.

The proposed solution improves the control dynamic performance and disturbance rejection. Then, it may help reducing the issues depending on control efforts, energy consumption to compensate disturbances. Moreover, the control architecture implies a simple updating of the usually employed elements (i.e., a FOPI replaces a PI controller and a fractional-order filter replaces a smoothing filter). The limitations could be determined by the practical implementation of the irrational transfer functions. The orders of realization, however, are kept low both in the controller and in the pre-filter.

The rest of the paper is organized as follows. Section II provides background on the considered electrical drives. Section III describes the approach to design the FOPI controller and Section IV illustrates the design of set-point pre-filters. Section V shows results of experimental tests. Finally, Section VI draws the conclusions.

II. The Modeled Electrical Systems

Many industrial loops employ permanent magnet DC-motors or permanent magnet synchronous motor (PMSM) drives. Hence, in this paper, these two systems are test beds for measuring the performance obtained by the proposed control architecture. This section briefly recalls the respective characteristics, properties, and operation and presents sufficiently accurate mathematical system models.

A. The DC-motor

The DC-motor armature voltage equations are given by:

$$v_a \;=\; R_a\,(1+T_a\,p)\,i_a + K_v\,\Phi\,\omega_r \tag{1}$$

where R_a, L_a, and $T_a \;=\; L_a/R_a$ are the armature winding resistance, inductance, and time constant, respectively; Φ is the constant excitation flux due to permanent magnets or independent field excitation winding; v_a, i_a and e_a are the armature voltage, current, and back-electromotive force, respectively; finally ω_r is the rotor speed, K_v is the voltage constant and $p \;=\; d/dt$. The mechanical equations are:

$$J\,p\,\omega_r \;=\; C_e - B\,\omega_r - C_L \;\;\text{and}\;\; p\,\theta_r \;=\; \omega_r \tag{2}$$

where $C_e \;=\; K_v\,\Phi\,i_a$ is the electromagnetic torque developed by the motor, J is the inertia moment of the rotor and connected load, B is the viscous friction coefficient, C_L is the external load torque, and θ_r is the rotor position. In the Laplace-transform s-domain, the previous equations become:

$$\begin{aligned} I_a \;&=\; \frac{\frac{1}{R_a}}{1+T_a\,s}\,(V_a - K_v\,\Phi\,\Omega_r) \\ \Omega_r &= \frac{1}{J\,s+B}\,(C_e - C_L) \Rightarrow \Theta_r = \frac{1}{s(Js+B)}(C_e - C_L). \end{aligned} \tag{3}$$

Taking into account the static friction, the mechanical model can be extended by including a pure time delay ϑ.

B. The PMSM Drive

The PMSM drives voltage equations in the d-q rotor reference frame are [21]:

$$\begin{aligned} v_{s,d} \;&=\; R_s\,i_{s,d} + L_{s,d}\,\frac{di_{s,d}}{dt} - \omega_r\,L_{s,q}\,i_{s,q} \\ v_{s,q} \;&=\; R_s\,i_{s,q} + L_{s,q}\,\frac{di_{s,q}}{dt} + \omega_r\,(L_{s,d}\,i_{s,d} + \Psi_{PM}) \end{aligned} \tag{4}$$

where $v_{s,d}$, $v_{s,q}$, $i_{s,d}$ and $i_{s,q}$ are the stator voltage and current vector d-q components, R_s is the resistance of each stator phase, $L_{s,d}$ and $L_{s,q}$ are the d- and q-axis stator inductances, Ψ_{PM} is the permanent magnet flux linked to the stator windings, and ω_r is the electrical motor speed.

The electromagnetic torque developed by the motor is:

$$C_e \;=\; 1.5\,n_p\,[\Psi_{PM}\,i_{s,q} + (L_{s,d} - L_{s,q})\,i_{s,q}\,i_{s,d}] \tag{5}$$

where n_p is the number of pole pairs. In case of superficial PMSM, magnetic isotropy leads to $L_{s,d} = L_{s,q}$. Then C_e does not contain the term due to saliency (reluctance torque):

$$C_e \;=\; 1.5\,n_p\,\Psi_{PM}\,i_{s,q} \;=\; K_c\,i_{s,q}. \tag{6}$$

Equations (4) show the dynamic coupling between the two axes. Independent control requires the coupling terms to be compensated by injecting feed-forward decoupling signals:

$$\begin{aligned} v_{s,dcomp} \;&=\; -\omega_r\,L_{s,q}\,i_{s,q} \\ v_{s,qcomp} \;&=\; \omega_r\,(L_{s,d}\,i_{s,d} + \Psi_{PM}). \end{aligned} \tag{7}$$

Thus the control system will give the reference signals of d-q voltages as follows:

$$\begin{aligned} v^*_{s,d} &= v_{s,d} + \omega_r L_{s,q} i_{s,q} = R_s i_{s,d} + L_{s,d}\frac{di_{s,d}}{dt} \\ v^*_{s,q} &= v_{s,q} - \omega_r(L_{s,d} i_{s,d} + \Psi_{PM}) = R_s i_{s,q} + L_{s,q}\frac{di_{s,q}}{dt}. \end{aligned} \tag{8}$$

In the Laplace-transform s-domain, (8) becomes:

$$\begin{aligned} V^*_{s,d} \;&=\; (R_s + L_{s,d}\,s)\,I_{s,d} \;=\; R_s\,(1+T_d\,s)\,I_{s,d} \\ V^*_{s,q} \;&=\; (R_s + L_{s,q}\,s)\,I_{s,q} \;=\; R_s\,(1+T_q\,s)\,I_{s,q} \end{aligned} \tag{9}$$

where $T_d \;=\; T_q$ for superficial PMSM.

The PMSM is controlled by two inner loops for the d- and q-axis current components, and an outer loop for rotor speed (Fig. 1). The d-axis current reference signal is set equal to zero, by the maximum torque per ampere criterion for a superficial PMSM. Moreover, time delays associated with several necessary operations are represented as first-order systems with small time constants. If T_c is the sampling period, delays are due to: signal sampling ($T_c/2$) and holding ($T_c/2$), inverter operation ($T_c/2$), computation of the control algorithm (T_c), and speed (τ_{sp}) and current (τ_L) measurement. Note that k_{inv} is the converter static gain. Fig. 2 shows the block diagram for both the d- and q- axis current control loops.

The open-loop transfer function of both the current control loops is simplified by considering an equivalent unitary feedback loop and by summing up all the small time constants in $\tau_{\Sigma i} = 5T_c/2 + \tau_L$. The current PI controller $G_{PI_{isq}}(s) = K_{isq}(1+\tau_{isq}s)/\tau_{isq}s$ is designed by applying the zero-pole cancelation to the plant pole and the absolute value optimum criterion [22]. The controller parameters are given by

$$\tau_{isq} \;=\; T_d \;=\; T_q \;\;\text{and}\;\; K_{isq} \;=\; \frac{R_s\,\tau_{isq}}{2\,k_{inv}\,\tau_{\Sigma i}} \tag{10}$$

and the closed-loop transfer function of the inner loop is

$$G_{0,isq}(s) \;=\; \frac{1}{1-\tau_L s}\;\frac{1}{1-\frac{T_c}{2}s}\;\frac{1}{1+2\,\tau_{\Sigma i}\,s+2\,\tau^2_{\Sigma i}\,s^2} \tag{11}$$

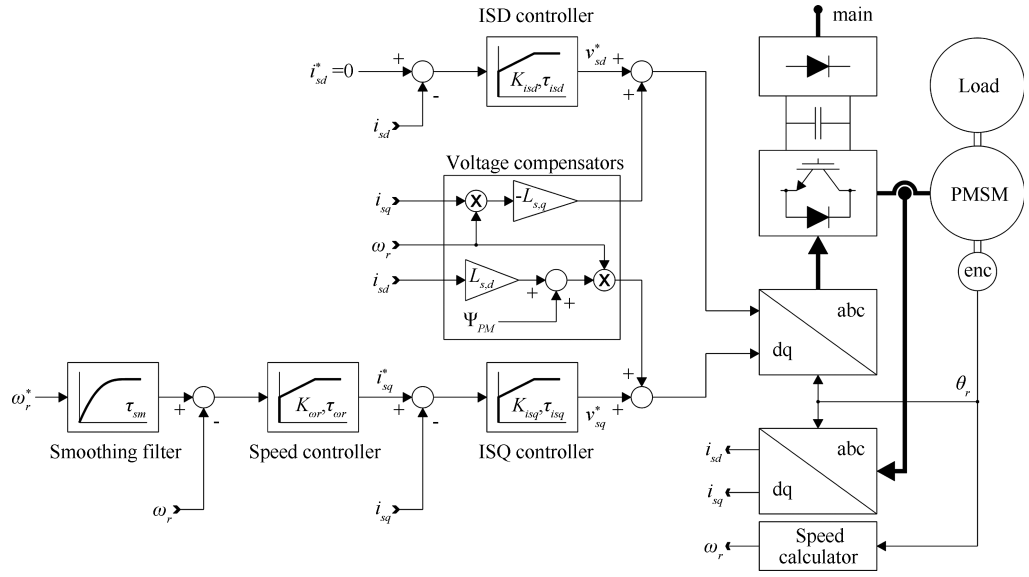

Fig. 1. Scheme of the vector controlled PMSM drive.

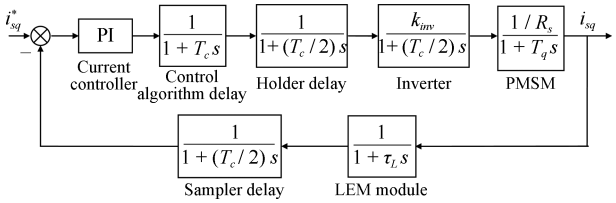

Fig. 2. Scheme of the q-axis current control loop.

where the first two factors respectively approximate $(1+\tau_L s)$ and $(1+T_c s/2)$. Namely, these last terms are originated by the equivalent representation with unitary feedback to include the time delays τ_L and $T_c/2$, respectively, in the forward path.

The block diagram implementing the speed control loop is shown in Fig. 3. The open-loop transfer function for speed control is simplified by neglecting the very small term $2\,\tau_{\Sigma i}^2\,s^2$ and by summing up all the small time constants $\tau_{\Sigma\omega} = 44\,T_c/2 + 44\,T_c - T_c/2 - \tau_L + 2\,\tau_{\Sigma i} + \tau_{sp}$. Note that the coefficients in the previous formula are determined by a sampling in the outer speed loop different from the inner current loop. Then the process transfer function is

$$G_{p,\omega r}(s) \;=\; \frac{K_c\,n_p}{J\,s\,(1+\tau_{\Sigma\omega}\,s)}. \tag{12}$$

The usual choice for speed control is to tune an integer-order PI controller $G_{PI_{\omega r}}(s) = K_{\omega r}(1+\tau_{\omega r}\,s)/\tau_{\omega r}\,s$ by the symmetrical optimum criterion [23], [24]. The method is based on tuning the controller parameters as:

$$\tau_{\omega r} \;=\; 4\,\tau_{\Sigma\omega} \;\text{ and }\; K_{\omega r} \;=\; \frac{J}{2\,\tau_{\Sigma\omega}\,K_c\,n_p}. \tag{13}$$

The word "symmetrical" refers to the obtained symmetry of the compensated Bode diagram with respect to the gain crossover. The word "optimum" refers to the higher ability of disturbance rejection. Moreover, a smoothing first order filter with a time constant in $(4\,\tau_{\Sigma\omega}, 4.8\,\tau_{\Sigma\omega})$ lowers the overshoot.

III. Fractional-order PI Controller Design

A. The Design Approach

The initial assumption is that both DC-motors and PMSM drives are modeled as first-order systems with an integrator

$$G_p(s) \;=\; \frac{K}{s\,(1+T\,s)} \tag{14}$$

which is common when controlling position of DC-motors (see (3)) and speed of PMSM drives (see (12)), respectively, and is suitable for many industrial applications. In case of DC-motor speed control, the plant transfer function is

$$G_p(s) \;=\; \frac{K}{1+T\,s}. \tag{15}$$

All the elements in the control loop introduce delays that are associated with an equivalent time constant, which is indicated by T and is obtained in Section II.

A fractional-order PI controller, FOPI for short, also named PI^ν controller, is used. The integrator is of non-integer order ν. A FOPI controller is chosen because it is the closest one to the standard integer-order PI controller that is applied in most industrial control loops. The FOPI transfer function is

$$G_c(s) \;=\; K_P + \frac{K_I}{s^\nu} \;=\; \frac{K_I\,(1+T_I\,s^\nu)}{s^\nu} \tag{16}$$

where K_P and K_I are the proportional and integral gain, respectively, and $T_I = K_P/K_I$. Moreover, the non-integer order is $1 < \nu < 2$, such that $1/s^\nu = (1/s)\cdot(1/s^\mu)$, with $\mu = \nu - 1$ and $0 < \mu < 1$. Then, the integer order integrator $1/s$ rejects common torque disturbances on the motor input, and the residual non-integer order integrator is given by the operator $1/s^\mu$. For practical implementation, the irrational transfer function is approximated as shown in Section III-B.

The open-loop transfer function $G(s) = G_c(s)\,G_p(s)$ is

$$G(s) \;=\; \begin{cases} a: \;\dfrac{K\,K_I\,(1+T_I s^\nu)}{s^{\nu+1}\,(1+Ts)} & \text{with plant (14)} \\ b: \;\dfrac{K\,K_I\,(1+T_I s^\nu)}{s^\nu\,(1+Ts)} & \text{with plant (15).} \end{cases} \tag{17}$$

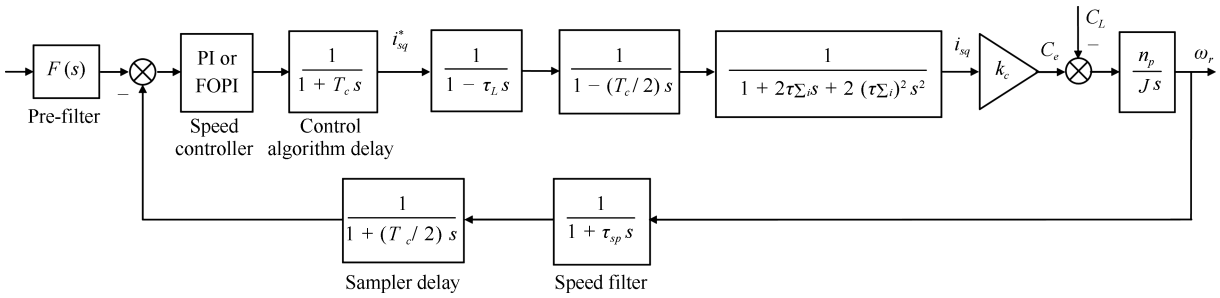

Fig. 3. Scheme of the speed control loop: the reference is given by the employed pre-filter, which is a smoothing one with an integer-order PI, an integer- or fractional-order pre-filter with a FOPI.

The controller is designed to obtain superior robustness to parametric variations and to achieve a nearly optimal feedback system [25]. Let us first consider the robustness requirement. To this aim, the non-integer integrator must lead to the fractal robustness. In other words, the open-loop frequency response (OLFR) must be characterized by a nearly flat phase diagram and a constant slope of the magnitude diagram in a sufficiently wide interval around the gain crossover frequency. To this aim, the fractional integrator provides a constant phase plot of $-\nu\pi/2$ and a magnitude plot with slope of -20ν dB/decade. Then replacing $s = j\omega$ yields the OLFR $G(j\omega)$ and the phase function $\angle G(j\omega)$ which must guarantee the robustness specification by imposing the desired phase margin at the crossover frequency, say ω_c. This ensures a stable performance despite parameter variations.

Regarding the optimality, consider the closed-loop frequency response $G_{cl}(j\omega) = 1/(1 + G^{-1}(j\omega))$. It is well-known that a feedback system is optimal if and only if the magnitude of the return difference $|1 + G^{-1}(j\omega)|$ is unitary for all frequencies [26]. In this condition, indeed, a perfect input/output tracking is achieved, whichever is the input signal. Unfortunately, this condition cannot be satisfied by real systems. Moreover, since $|G(j\omega)| \gg 1$ may lead to instability, the OLFR is shaped around ω_c so that the gain is high at low frequency and rolls off at high frequency. Then, the optimal requirement is only approximated in a specified bandwidth, say ω_B, in which it is desired to achieve a good tracking performance.

To start with, consider the OLFR given by

$$G(j\omega) = \begin{cases} a: \dfrac{K\,K_I\,[1 + T_I\,\omega^{\nu}\,(C + j\,S)]}{\omega^{\nu+1}(-S + j\,C)\,(1 + j\omega T)} \\ b: \dfrac{K\,K_I\,[1 + T_I\,\omega^{\nu}\,(C + j\,S)]}{\omega^{\nu}\,(C + j\,S)\,(1 + j\,\omega\,T)} \end{cases} \tag{18}$$

with $C = \cos(\pi\nu/2)$ and $S = \sin(\pi\nu/2)$, which can be expressed in terms of a normalized angular frequency $\overline{\omega} = \omega T$:

$$G(j\overline{\omega}) = \begin{cases} a: \dfrac{K\,K_I\,\left[1 + T_I\,\left(\frac{\overline{\omega}}{T}\right)^{\nu}\,(C + j\,S)\right]}{\left(\frac{\overline{\omega}}{T}\right)^{\nu+1}\,(-S + j\,C)\,(1 + j\,\overline{\omega})} \\ b: \dfrac{K\,K_I\,\left[1 + T_I\,\left(\frac{\overline{\omega}}{T}\right)^{\nu}\,(C + j\,S)\right]}{\left(\frac{\overline{\omega}}{T}\right)^{\nu}\,(C + j\,S)\,(1 + j\,\overline{\omega})}. \end{cases} \tag{19}$$

Then the magnitude of the OLFR is given by

$$|G(j\overline{\omega})| = \begin{cases} a: \dfrac{K\,K_I}{\left(\frac{\overline{\omega}}{T}\right)^{\nu+1}} \sqrt{\dfrac{1 + 2\,T_I\,\left(\frac{\overline{\omega}}{T}\right)^{\nu}\,C + T_I^2\,\left(\frac{\overline{\omega}}{T}\right)^{2\nu}}{1 + \overline{\omega}^2}} \\ b: \dfrac{K\,K_I}{\left(\frac{\overline{\omega}}{T}\right)^{\nu}} \sqrt{\dfrac{1 + 2\,T_I\,\left(\frac{\overline{\omega}}{T}\right)^{\nu}\,C + T_I^2\,\left(\frac{\overline{\omega}}{T}\right)^{2\nu}}{1 + \overline{\omega}^2}} \end{cases} \tag{20}$$

and the phase of the OLFR is given by

$$\angle G(j\overline{\omega}) = \begin{cases} a: \varphi_1(\overline{\omega}) - \varphi_2(\overline{\omega}) - \dfrac{\pi(\nu+1)}{2} \\ b: \varphi_1(\overline{\omega}) - \varphi_2(\overline{\omega}) - \dfrac{\pi\nu}{2} \end{cases} \tag{21}$$

where $\varphi_1(\overline{\omega}) = \tan^{-1}\left(T_I S\left(\frac{\overline{\omega}}{T}\right)^{\nu}/(1 + T_I C\left(\frac{\overline{\omega}}{T}\right)^{\nu})\right)$ and $\varphi_2(\overline{\omega}) = \tan^{-1}(\overline{\omega})$.

Now, the design procedure begins with choosing the bandwidth $\overline{\omega}_B = \omega_B T$ where input/output tracking is desired. The value $\overline{\omega}_B$ is chosen higher than the plant bandwidth. Moreover, as it will be shown below, the integral time constant T_I depends on $\overline{\omega}_B$. So, $T_I > 0$ must hold true for a stable controller. More in details, $\overline{\omega}_B$ was maximized after a trial-and-error procedure. It is also remarked that maximizing $\overline{\omega}_B$ reduces the rise time of the closed-loop response, but it also increases the crossover $\overline{\omega}_c$, which could be shifted too much with respect to a centered position in the range where the phase diagram is flat or slowly changing. Then, a tradeoff must be reached between performance and robustness, as it is usual.

Next, the crossover $\overline{\omega}_c$ is determined by a relation that is commonly used for estimation: $\overline{\omega}_c \in [\overline{\omega}_B/1.7, \overline{\omega}_B/1.3]$ [27], e.g., $\overline{\omega}_c = \overline{\omega}_B/1.5$, but this interval allows changing the value of $\overline{\omega}_c$. Obviously, other methods can be used to set $\overline{\omega}_c$.

Hence, the phase margin specification is enforced as a robustness measure. Since $PM = \pi + \angle G(j\overline{\omega}_c)$, it holds

$$PM = \begin{cases} a: \varphi_1(\overline{\omega}_c) - \varphi_2(\overline{\omega}_c) + \dfrac{\pi(1-\nu)}{2} \\ b: \varphi_1(\overline{\omega}_c) - \varphi_2(\overline{\omega}_c) + \dfrac{\pi(2-\nu)}{2}. \end{cases} \tag{22}$$

Now, $\varphi_1(\overline{\omega}_c) - \varphi_2(\overline{\omega}_c) = \pi/2$ is set in case a or $\varphi_1(\overline{\omega}_c) - \varphi_2(\overline{\omega}_c) = 0$ is set in case b. These settings introduce a constraint on T_I but give the advantage of a strict, closed-form, and simple relation between the specified phase margin and the required fractional order. Namely, in both cases a and b, the

previous settings yield $PM = \pi(2-\nu)/2$. If the specification PM_s is given, then the following relation is established

$$PM_s = (2-\nu)\pi/2 \Leftrightarrow \nu = 2 - 2PM_s/\pi. \tag{23}$$

The introduced constraint yields a closed-form expression that is used as tuning rule for the integral time constant:

$$T_I = \begin{cases} a: \dfrac{-1}{\left(\dfrac{\overline{\omega}_c}{T}\right)^{\nu}(S\,\overline{\omega}_c + C)} \\ b: \dfrac{\overline{\omega}_c}{\left(\dfrac{\overline{\omega}_c}{T}\right)^{\nu}(S - \overline{\omega}_c\, C)}. \end{cases} \tag{24}$$

To set the remaining parameter K_I, the condition $|G^{-1}(j\overline{\omega}_c)|^2 = 1$ uses the gain crossover normalized angular frequency $\overline{\omega}_c$ and leads to another closed-form expression that is exploited as a rule for the integral gain:

$$K_I = \begin{cases} a: \dfrac{1}{K}\left(\dfrac{\overline{\omega}_c}{T}\right)^{\nu+1}\sqrt{\dfrac{1+\overline{\omega}_c^2}{1+2\,T_I\,\left(\frac{\overline{\omega}_c}{T}\right)^{\nu}\,C + T_I^2\,\left(\frac{\overline{\omega}_c}{T}\right)^{2\nu}}} \\ b: \dfrac{1}{K}\left(\dfrac{\overline{\omega}_c}{T}\right)^{\nu}\sqrt{\dfrac{1+\overline{\omega}_c^2}{1+2\,T_I\,\left(\frac{\overline{\omega}_c}{T}\right)^{\nu}\,C + T_I^2\,\left(\frac{\overline{\omega}_c}{T}\right)^{2\nu}}} \end{cases} \tag{25}$$

in which T_I is the value given by (24). The proportional gain is $K_P = K_I\,T_I$.

If the plant includes a pure time delay ϑ, i.e., $G_p(s)$ of (14) and (15) is replaced by $G_p(s)\,e^{-\vartheta s}$, or if the control loop is affected by a significant dead-time ϑ, the OLFR becomes $G(j\overline{\omega})\,e^{-j\overline{\omega}\vartheta/T}$. For example, as already mentioned in Section II-A, it is necessary to model the static friction effect of the DC-motor. In this case, the design procedure is easily extended. Namely, the magnitude does not change, whereas the argument is modified as

$$\angle G(j\overline{\omega}) = \begin{cases} a: \varphi_1(\overline{\omega}) - \varphi_2(\overline{\omega}) - \dfrac{\pi\,(\nu+1)}{2} - \dfrac{\overline{\omega}\,\vartheta}{T} \\ b: \varphi_1(\overline{\omega}) - \varphi_2(\overline{\omega}) - \dfrac{\pi\,\nu}{2} - \dfrac{\overline{\omega}\,\vartheta}{T} \end{cases} \tag{26}$$

then the phase margin becomes

$$PM = \begin{cases} a:\ \varphi_1(\overline{\omega}_c) - \varphi_2(\overline{\omega}_c) + \dfrac{\pi\,(1-\nu)}{2} - \dfrac{\overline{\omega}_c\,\vartheta}{T} \\ b:\ \varphi_1(\overline{\omega}_c) - \varphi_2(\overline{\omega}_c) + \dfrac{\pi\,(2-\nu)}{2} - \dfrac{\overline{\omega}_c\,\vartheta}{T}. \end{cases} \tag{27}$$

In this case, the settings are $\varphi_1(\overline{\omega}_c) - \varphi_2(\overline{\omega}_c) - \overline{\omega}_c\vartheta/T = \pi/2$ in case a and $\varphi_1(\overline{\omega}_c) - \varphi_2(\overline{\omega}_c) - \overline{\omega}_c\vartheta/T = 0$ in case b. The formulas for T_I are updated as follows:

$$T_I = \begin{cases} a: \dfrac{\overline{\omega}_c\gamma - 1}{\left(\dfrac{\overline{\omega}_c}{T}\right)^{\nu}[(\gamma + \overline{\omega}_c)S + (1 - \gamma\overline{\omega}_c)C]} \\ b: \dfrac{\overline{\omega}_c + \gamma}{\left(\dfrac{\overline{\omega}_c}{T}\right)^{\nu}[(1 - \gamma\overline{\omega}_c)S - (\overline{\omega}_c + \gamma)C]} \end{cases} \tag{28}$$

where $\gamma = \tan(\overline{\omega}_c\vartheta/T)$. Note that (28) coincides with (24) when $\vartheta \to 0$. Since the magnitude keeps unchanged, the crossover specification sets the integral gain by the same rule (25).

B. Realization of the FOPI Controller

The final step in the synthesis procedure is to realize the FOPI transfer function. Namely, in (16) the irrational operator s^{ν} requires an approximation as rational transfer function. Literature discloses several methods [11], [13], [28]−[30]. Here, a methodology is employed to a priori guarantee that zeros and poles of the rational transfer function are interlaced with each other in the negative real half-axis of the s-plane [31], [32]. This method warrants stability and minimum-phase properties, that are important for control purpose. Finally, it is based on closed-form formulas that can be easily applied to obtain the coefficients of the rational transfer function, depending on ν and the number N of zero-pole pairs in the approximation. The greater is N, the better is the approximation of s^{ν}, but also the more complex and memory-demanding is the implementation. More precisely, a continued fractions expansion is truncated and converted to a rational transfer function

$$s^{\lambda} \approx \frac{\alpha_{N,0}(\lambda)\,s^N + \alpha_{N,1}(\lambda)\,s^{N-1} + \cdots + \alpha_{N,N}(\lambda)}{\beta_{N,0}(\lambda)\,s^N + \beta_{N,1}(\lambda)\,s^{N-1} + \cdots + \beta_{N,N}(\lambda)} \tag{29}$$

where $0 < \lambda < 1$, $N \geq 1$ is the number of zero-pole interlaced pairs and the coefficients $\alpha_{N,j}(\lambda) = \beta_{N,N-j}(\lambda)$, for $j = 0, \ldots, N$, depend on λ. The coefficients can be computed very easily and rapidly by a closed-form formula:

$$\alpha_{N,j}(\lambda) = (-1)^j \binom{N}{j} (\lambda + j + 1)_{(N-j)} (\lambda - N)_{(j)} \tag{30}$$

in which $(\lambda+j+1)_{(N-j)} = (\lambda+j+1)(\lambda+j+2)\cdots(\lambda+N)$ and $(\lambda-N)_{(j)} = (\lambda-N)(\lambda-N+1)\cdots(\lambda-N+j-1)$, with $(\lambda+N+1)_{(0)} = (\lambda-N)_{(0)} = 1$. Simple algebraic manipulations lead to [33], [34]:

$$\alpha_{N,j} = C(N,j)\,(j+1+\lambda)_{(N-j)}\,(N-\lambda)_{(j)^*} \tag{31}$$

$$\beta_{N,j} = C(N,j)\,(N-j+1+\lambda)_{(j)}\,(N-\lambda)_{(N-j)^*} \tag{32}$$

where $(N-\lambda)_{(j)^*} := (N-\lambda)(N-\lambda-1)\cdots(N-\lambda-j+1)$ and $(N-\lambda)_{(N-j)^*} := (N-\lambda)(N-\lambda-1)\cdots(j-\lambda+1)$ are falling factorials, with $(N-\lambda)_{(0)^*} = 1$. Similar methods and considerations can be applied for digital realizations [35]−[38].

IV. Set-point Pre-filter Design

To improve the set-point following performance, the design is completed by adding a suitable set-point pre-filter. The filter $F(s)$ is designed by the method recently proposed in [39], which is briefly revisited here for the reader's convenience and suitably adapted for the considered problem, where a feedback filter has to be taken into account.

The control loop includes the designed fractional-order PI controller, $G_c(s)$, a linear time-invariant commensurate strictly proper minimum-phase system, that can be of integer or non-integer order (a fractional system), and a possible feedback filter $R(s)$. The set-point pre-filter $F(s)$ aims at obtaining, independently from $G_c(s)$, an output transition as close as possible to a desired output function, that is a smooth and monotonic transition from an initial steady-state value to a new one in a finite time interval τ. The first step is to employ the

technique in [40] to synthesize a suitable command signal $r(t)$ that provides a perfect tracking of the desired output function. The second step is to find an integer or non-integer (fractional) pre-filter $F(s)$ that is able to provide a step response as close as possible, in terms of 2-norm, to the synthesized $r(t)$.

The synthesis of $r(t)$ is as follows [40]. The desired output signal $\bar{y}(t;\tau)$ was proposed in [41]. It can be represented, together with its fractional differintegral, as in (33)

$$D^{\alpha}\bar{y}(t;\tau) = \begin{cases} 0, & t<0 \\ \dfrac{(2n+1)!}{n!\tau^{2n+1}}\displaystyle\sum_{r=0}^{n}\frac{(-1)^{n-r}\tau^{r}(2n-r)!\,t^{2n-r+1-\alpha}}{r!(n-r)!\Gamma(2n-r+2-\alpha)} & t\le\tau \\ \dfrac{(2n+1)!}{n!\tau^{2n+1}}\displaystyle\sum_{r=0}^{n}\frac{(-1)^{n-r}\tau^{r}(2n-r)!}{r!(n-r)!} & \\ \times\left(\dfrac{t^{2n-r+1-\alpha}}{\Gamma(2n-r+2-\alpha)}-\displaystyle\sum_{j=0}^{n-r}\frac{\tau^{j}t^{2n-r+1-j-\alpha}}{j!\Gamma(2n-r+2-j-\alpha)}\right) & t>\tau \end{cases} \tag{33}$$

where $-\infty<\alpha\le n+1$. The previous τ-parameterized signal exhibits a smooth monotonic transition from 0 to 1 in a finite time interval τ and its degree of regularity is C^n.

To compute a command signal $r(t)$ such that a perfect tracking of the τ-parameterized output function $\bar{y}(t;\tau)$ is obtained, the open-loop transfer function $G(s)=G_c(s)G_p(s)$ is first considered. The input-output technique in [40] is straightforwardly applied to $G(s)$ (or to the delay-free part $\bar{G}$ of $G(s)=\bar{G}(s)e^{-\vartheta s}$ if there is a pure time delay ϑ in the loop), yielding the signal

$$\begin{aligned} r_{ol}(t;\tau) =& \gamma_{n-m}D^{\rho}\bar{y}(t;\tau)+\gamma_{n-m-1}D^{\rho-\nu}\bar{y}(t;\tau) \\ &+\cdots+\gamma_1 D^{\nu}\bar{y}(t;\tau)+\gamma_0\bar{y}(t;\tau) \\ &+\int_0^t \eta_0(t-\xi)\bar{y}(\xi;\tau)d\xi \end{aligned} \tag{34}$$

where ρ is the relative order of the open-loop transfer function and $\eta_0(t)$ is its zero order dynamics. Then, a correction term $r_c(t;\tau)=\mathcal{L}^{-1}[R(s)\bar{Y}(s;\tau)e^{-\vartheta s}]$ must be considered, so that the ideal command signal is

$$r(t;\tau) \;=\; r_{ol}(t;\tau)+r_c(t;\tau). \tag{35}$$

Details on the computation of (35), together with the proof of existence of the command signal, can be found in [40].

A. Transition Polynomial-Based Filter

The first method proposed for designing the set-point pre-filter $F(s)$ relies on the design of a transfer function whose step response is as close as possible (in terms of 2-norm) to the transition polynomial. The following transfer function structure is employed

$$\tilde{F}(s)=\frac{1}{\displaystyle\sum_{i=1}^{o}a_i s^i+1} \tag{36}$$

where $o=n+1$, so that the pre-filter step response exhibits the same degree of regularity of the transition polynomial. By sampling at each Δt the transition polynomial and its derivatives obtained via (33), the following matrices are created

$$A=\begin{bmatrix} D^o\bar{y}(0;\tau) & \cdots & D^1\bar{y}(0;\tau) \\ \vdots & & \vdots \\ D^o\bar{y}(t-\Delta t;\tau) & \cdots & D^1\bar{y}(t-\Delta t;\tau) \\ D^o\bar{y}(t;\tau) & \cdots & D^1\bar{y}(t;\tau) \\ D^o\bar{y}(t+\Delta t;\tau) & \cdots & D^1\bar{y}(t+\Delta t;\tau) \\ \vdots & \ddots & \vdots \\ D^o\bar{y}(3\tau;\tau) & \cdots & D^1\bar{y}(3\tau;\tau) \end{bmatrix} \tag{37}$$

$$B=\begin{bmatrix} 1(0)-\bar{y}(0;\tau) \\ \vdots \\ 1(t-\Delta t)-\bar{y}(t-\Delta t;\tau) \\ 1(t)-\bar{y}(t;\tau) \\ 1(t+\Delta t)-\bar{y}(t+\Delta t;\tau) \\ \vdots \\ 1(3\tau)-\bar{y}(3\tau;\tau) \end{bmatrix}. \tag{38}$$

Finally, the coefficients vector $\Theta=[a_o\cdots a_1]^T$ is obtained as $\Theta = A^T(AA^T)^{-1}B$. Now, using (36) and the process dynamics, the set-point pre-filter is designed as

$$F(s) \;=\; \tilde{F}(s)(R(s)e^{-\vartheta s}+\bar{G}^{-1}(s)) \tag{39}$$

where $\bar{G}^{-1}(s)$ is obtained straightforwardly by considering that $\bar{G}(s)$ is the delay free-part of the process. Moreover, it is worth stressing that, given the properness of $\tilde{F}(s)$, the overall filter $F(s)$ is always proper. Note that, in this case, the obtained filter is fractional. If a unitary-feedback loop is considered with no time delay, then $F(s) = \tilde{F}(s)(1+\bar{G}^{-1}(s))$.

B. Command Signal Filter

The second methodology for designing the set-point pre-filter $F(s)$ is based on the direct design of an integer order pre-filter whose step response is the closest, in terms of 2-norm, to the command signal (35). The proposed filter structure is

$$F(s) \;=\; \frac{\displaystyle\sum_{j=1}^{o-p}b_j s^j+1}{\displaystyle\sum_{i=1}^{o}a_i s^i+\mu} \tag{40}$$

where μ is the closed-loop dc-gain, $p=n-[\rho_G]$, with ρ_G the relative order of the open-loop transfer function, and $o\in\mathbb{R}$ is a design parameter. In this case, the identification would require $o-p$ differentiation of the step signal. To overcome this problem, both the step and the command signals are integrated $o-p$ times yielding (41)–(42), shown at the bottom of the next page.

Finally, the coefficients vector is defined as $\Theta = [a_o\ \cdots\ a_1\ b_{o-p}\ \cdots b_1]^T$ and is obtained by the same formula $\Theta = A^T(AA^T)^{-1}B$.

V. Experimental Validation

In this section, the proposed control scheme combining a feedback FOPI controller and a set-point pre-filter is tested. It is also compared with an industrial solution, combining a PI controller, which is tuned by the classical symmetrical optimum method, and a smoothing pre-filter. The tests are done by simulation of identified input/output models and by experiments performed on real equipment. Two different test beds are considered.

The first one is a 370 W brushed DC-servomotor (AMIRA DR300), that is driven by a device equipped with a power supply, a servo amplifier, a signal adaption unit, and a module for measuring outputs. PC-commands to the device are processed and sent by an interface board (a floating point 250 Mhz Motorola PPC dSPACE board DS1104). Then, all control functions can be generated directly by the PC which integrates the board. A 1024 pulses digital incremental encoder is mounted at the motor free drive-shaft to measure rotor position or speed. Feedback from the encoder arrives the board processor, that computes and sends the control action to the power unit. The board uses 16 bit A/D-D/A converters to process signals and commands, generates the position and speed references, applies the Euler's discretization rule and runs the controllers in discrete time. The PI or FOPI controllers and the set-point pre-filters are part of a Simulink block diagram the board uses to directly control the real plant or its I/O model. The board compiles the Simulink scheme, generates a real-time executable code, and downloads it to the board memory. Fig. 4 shows all the experimental set-up. The plant parameters are identified by a frequency-domain technique as: $K = 0.9843$, $T = 0.0651\,\text{s}$, $\vartheta = 0.02\,\text{s}$. Then, formulas (28) and (25) are used to design the FOPI controller.

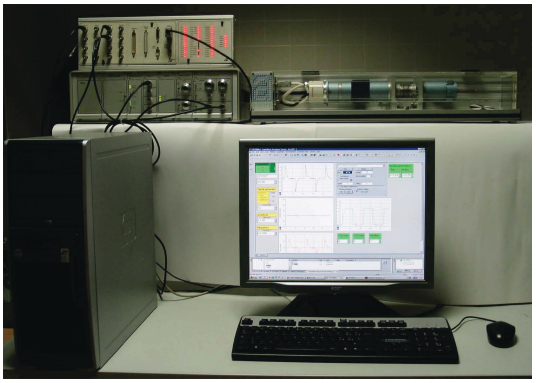

Fig. 4. Experimental set-up for controlling the DC-servomotor.

The second test bed system is a PMSM drive (SIEMENS series 1FK7 CT) with the characteristics and parameters shown in Table I. This system is tested by the experimental set-up in Fig. 5. The diagram in Fig. 1 accurately represents the controlled system. If $T_c = 0.1\,\text{ms}$, $\tau_{sp} = 6 \cdot 10^{-6}\,\text{ms}$, and $\tau_L = 0.7\,\text{ms}$, then $\tau_{\Sigma i} = 0.95\,\text{ms}$ and the Absolute Value Optimum Criterion settings provide $\tau_{isq} = 0.0114\,\text{s}$ and $K_{isq} = 6.5253$ for the current PI controller. Moreover, for the

$$A = \begin{bmatrix} D^p r(0;\tau) & \cdots & D^{-o+p+1} r(0;\tau) & \cdots & -1(0) & \cdots & -\dfrac{1}{(o-p+1)!}0^{(o-p+1)} \\ \vdots & \ddots & \vdots & \ddots & \vdots & \ddots & \vdots \\ D^p r(t-\Delta t;\tau) & \cdots & D^{-o+p+1} r(t-\Delta t;\tau) & \cdots & -1(t-\Delta t) & \cdots & -\dfrac{1}{(o-p+1)!}(t-\Delta t)^{(o-p+1)} \\ D^p r(t;\tau) & \cdots & D^{-o+p+1} r(t;\tau) & \cdots & -1(t) & \cdots & -\dfrac{1}{(o-p+1)!}t^{(o-p+1)} \\ D^p r(t+\Delta t;\tau) & \cdots & D^{-o+p+1} r(t+\Delta t;\tau) & \cdots & -1(t+\Delta t) & \cdots & -\dfrac{1}{(o-p+1)!}(t+\Delta t)^{(o-p+1)} \\ \vdots & \ddots & \vdots & \ddots & \vdots & \ddots & \vdots \\ D^p r(3\tau;\tau) & \cdots & D^{-o+p+1} r(3\tau;\tau) & \cdots & -1(3\tau) & \cdots & -\dfrac{1}{(o-p+1)!}(3\tau)^{(o-p+1)} \end{bmatrix} \tag{41}$$

$$B = \begin{bmatrix} \dfrac{1}{(o-p)!}0^{(o-p)} - \mu D^{-o+p} r(0;\tau) \\ \vdots \\ \dfrac{1}{(o-p)!}(t-\Delta t)^{(o-p)} - \mu D^{-o+p} r(t-\Delta t;\tau) \\ \dfrac{1}{(o-p)!}t^{(o-p)} - \mu D^{-o+p} r(t;\tau) \\ \dfrac{1}{(o-p)!}(t+\Delta t)^{(o-p)} - \mu D^{-o+p} r(t+\Delta t;\tau) \\ \vdots \\ \dfrac{1}{(o-p)!}(3\tau)^{(o-p)} - \mu D^{-o+p} r(3\tau;\tau) \end{bmatrix} \tag{42}$$

speed loop, the I/O plant model parameters in (12) are $K = K_c n_p/J = 728.5343$ and $T = \tau_{\Sigma\omega} = 0.0078\,\text{s}$. Then, for the PI designed with the Symmetrical Optimum Criterion, $\tau_{\omega r} = 0.0310\,\text{s}$ and $K_{\omega r} = 0.0886$. Whereas, formulas (24) and (25) (case a) are used to design the FOPI controller.

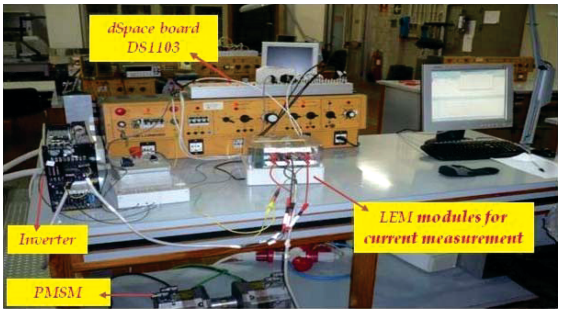

Fig. 5. Experimental set-up for controlling the PMSM drive.

A. First Case: Control of DC-motor

The control approach is applied both to the position and speed of the DC-motor. The tests are performed both in simulation and by experiments. Simulation employs the models $G_p(s) = K\,e^{-\vartheta\,s}/(s\,(1+T\,s))$ for position control and $G_p(s) = K\,e^{-\vartheta\,s}/(1+T\,s)$ for speed control. Experiments are made by directly applying the controllers to the real system through the dSpace board.

As basis for comparison, a PI controller, that is tuned by the symmetrical optimum method (for position control) or by the absolute value optimum criterion (for speed control) with a smoothing pre-filter, is applied. On the other side, the FOPI controller is designed by (28) and (25). For robustness specifications, the fractional orders $\nu = 1.4, 1.5, 1.6$ are used as good trade-off values respectively providing the phase margins $54°, 45°, 36°$ by (23). Moreover, the performance specifications are $\overline{\omega}_c = 0.5$, for position control, and $\overline{\omega}_c = 1.8$, for speed control. The designed values of the controller gains are shown in Table II. All the FOPI controllers are realized by rational transfer functions with $N = 5$ zero-pole pairs. Finally, the integer-order and fractional-order pre-filters are designed by the method in Section IV.

TABLE I
PMSM NAME PLATE DATA AND PARAMETERS

Description	Value (Measure unit)
Nominal power	2.14 (KW)
Nominal current	4.40 (A)
Nominal torque	6.80 (Nm)
Power factor ($\cos(\varphi)$)	0.80
Frequency	200 (Hz)
Nominal speed	3000 (rpm)
No. of pole pairs	4
Stator resistance: R_s	1.09 (Ω)
d- & q- axis inductances: L_{sd}, L_{sq}	12.4, 12.4 (mH)
Inertia moment: J	0.006 (Kg m^2)
Viscous friction coefficient: B	0 (0.05) (Nms)
Permanent magnets flux: Ψ_{PM}	0.1821 (Wb)
Torque constant: K_c	1.0928 (Nm/A)

Fig. 6 shows the reference step responses both for position control (above) and for speed control (below), corresponding to the selected values of ν. Moreover, the response to speed reversal and to load application is shown in the same figure. The responses obtained with PI control are green, the ones obtained with FOPI control and an integer-order pre-filter are blue, and the ones with FOPI control and a fractional-order

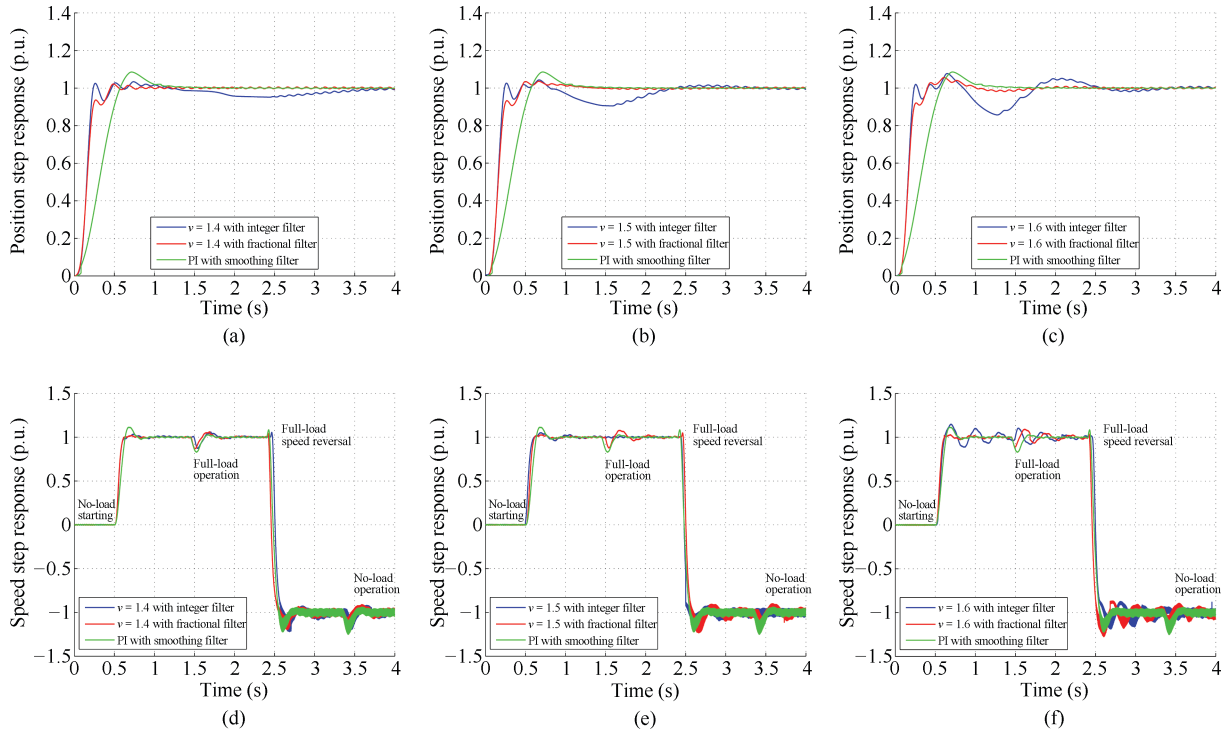

Fig. 6. PI and FOPI control of DC-motor position and speed: PI with smoothing filter (green), FOPI with integer-order (blue) or fractional-order filters (red).

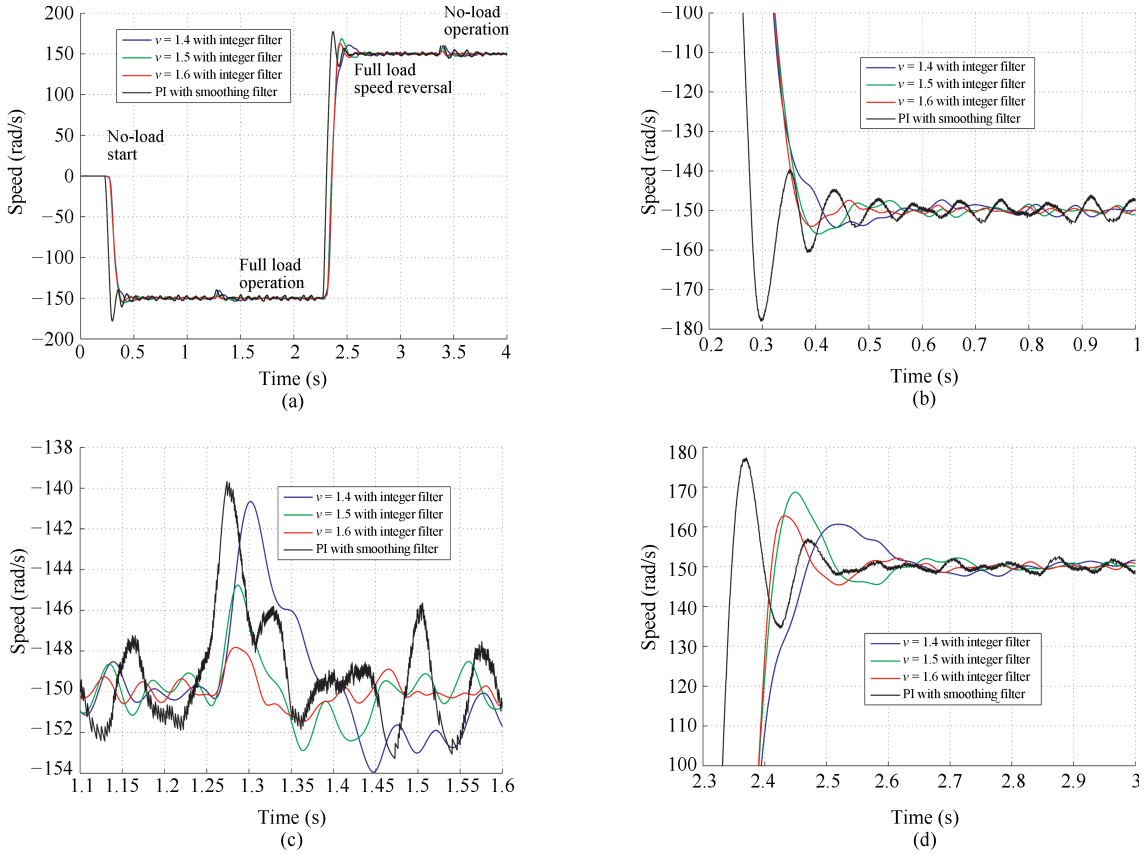

Fig. 7. Control of the speed of a PMSM by FOPI controllers and integer filters. (a) General view. (b) Zoom in the no-load start period. (c) Zoom in the full load operational period. (d) Zoom in the period after full load speed reversal.

pre-filter are red. Only experimental results are shown, namely simulation matches the experiments to a large extent.

TABLE II
FOPI CONTROLLER GAINS FOR DC-MOTOR AND PMSM DRIVES

	DC position control		DC speed control		PMSM Speed control	
ν	K_P	K_I	K_P	K_I	K_P	K_I
1.4	8.7936	2.0706	2.5831	148.3770	0.1314	5.9296
1.5	10.0609	43.9481	2.9554	289.8783	0.2004	29.7201
1.6	12.1033	123.7699	3.5553	563.3830	0.3616	119.5887

It is remarkable that the fractional pre-filters almost cancel the oscillations. The improvement is even more relevant in the case of speed control. The overshoot is greatly reduced and the settling and rise times are also reduced with respect to the PI-controlled system. Disturbance is better rejected by the FOPI with fractional filters that show a fast settling. The performance obtained by PI or FOPI when speed is reverted is comparable. This last result is due to the opposite action of the brushes when the sense of rotation is not the preferred one. Regarding the effect of changes in ν, the oscillations increase with ν (the phase margin decreases according to (23)).

B. Second Case: Control of PMSM Drive

Now the PMSM speed is controlled. The model is given by (14). Then, (24) and (25) are used for design purpose. Again, the orders $\nu = 1.4, 1.5, 1.6$ are chosen. Moreover, the desired performance is specified by the maximum bandwidth $\overline{\omega}_B$ that allows $T_I > 0$: by $\overline{\omega}_c = \overline{\omega}_B/1.7$, the necessary values are $\overline{\omega}_c = 0.6$ ($\overline{\omega}_B = 1.02$) for $\nu = 1.4$, $\overline{\omega}_c = 0.8$ ($\overline{\omega}_B = 1.36$) for $\nu = 1.5$, and $\overline{\omega}_c = 1.2$ ($\overline{\omega}_B = 2.04$) for $\nu = 1.6$. The values of the controllers' gains are shown in Table II and realization is by $N = 5$ zero-pole pairs.

To execute a suitable and intense test to verify performance and robustness, a reference step input of -150 rad/s (half of the rated speed) is first applied at $t = 0.225$ s. Then, an operation period follows in which a load disturbance of 2.2 Nm is superposed at $t = 1.253$ s. The motion is reverted at $t = 2.268$ s. Finally, the load is removed at $t = 3.361$s. The control scheme combining a FOPI controller and an integer/fractional pre-filter is compared with the traditional scheme that combines a smoothing pre-filter and a PI controller tuned by the symmetrical optimum method [23], [24]. Note that, in both schemes, the internal current loop includes the PI controller tuned by the absolute value optimum criterion. Figs. 7(a) and 8(a) show a general view of the entire test duration with integer filters and fractional filters, respectively.

First of all, the performance analysis of the reference step response without load applied, at the start of the operational test (see zoom in Figs. 7(b) and 8(b), is considered. The FOPI controllers provide a reasonable fast response and small overshoot with respect to the PI controller, especially with $\nu = 1.6$ and with fractional filters on the set-point (Fig. 8(b)).

In all the cases employing integer or fractional filters, improvements are obtained. Namely, the responses provided by the PI controller with a smoothing filter show lower rise

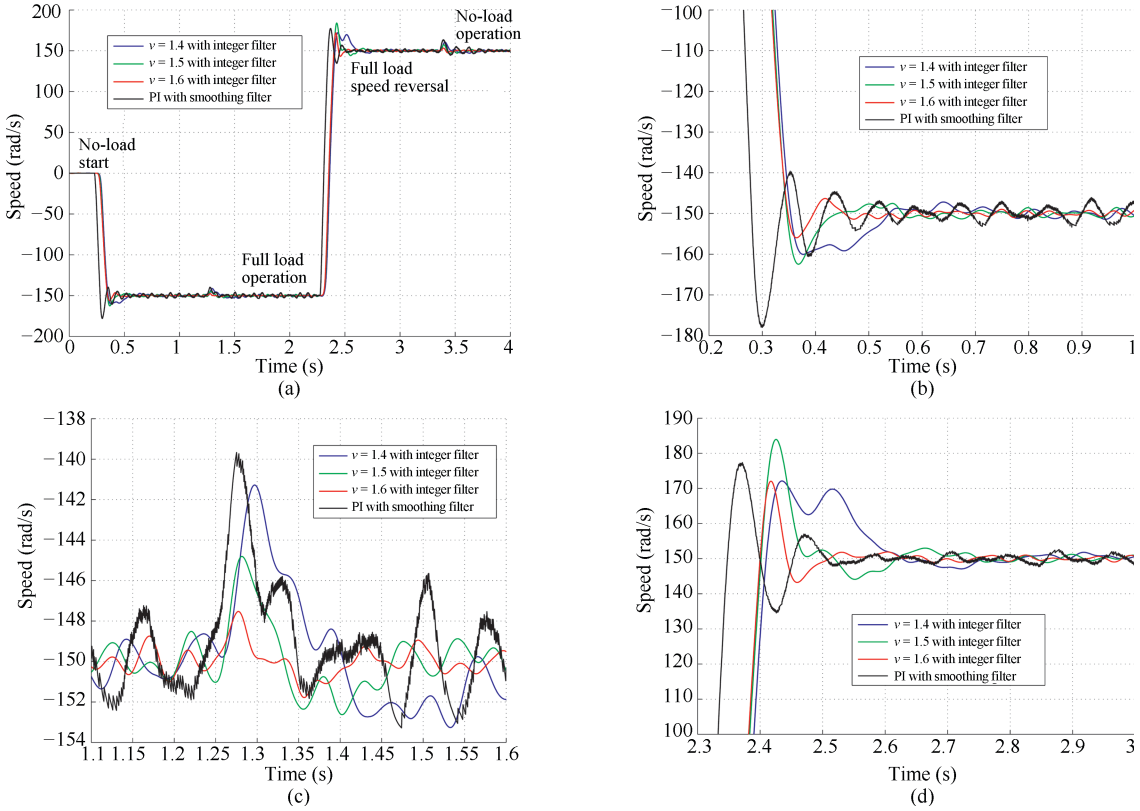

Fig. 8. Control of the speed of a PMSM by FOPI controllers and fractional filters. (a) General view. (b) Zoom in the no-load start period. (c) Zoom in the full load operational period. (d) Zoom in the period after full load speed reversal.

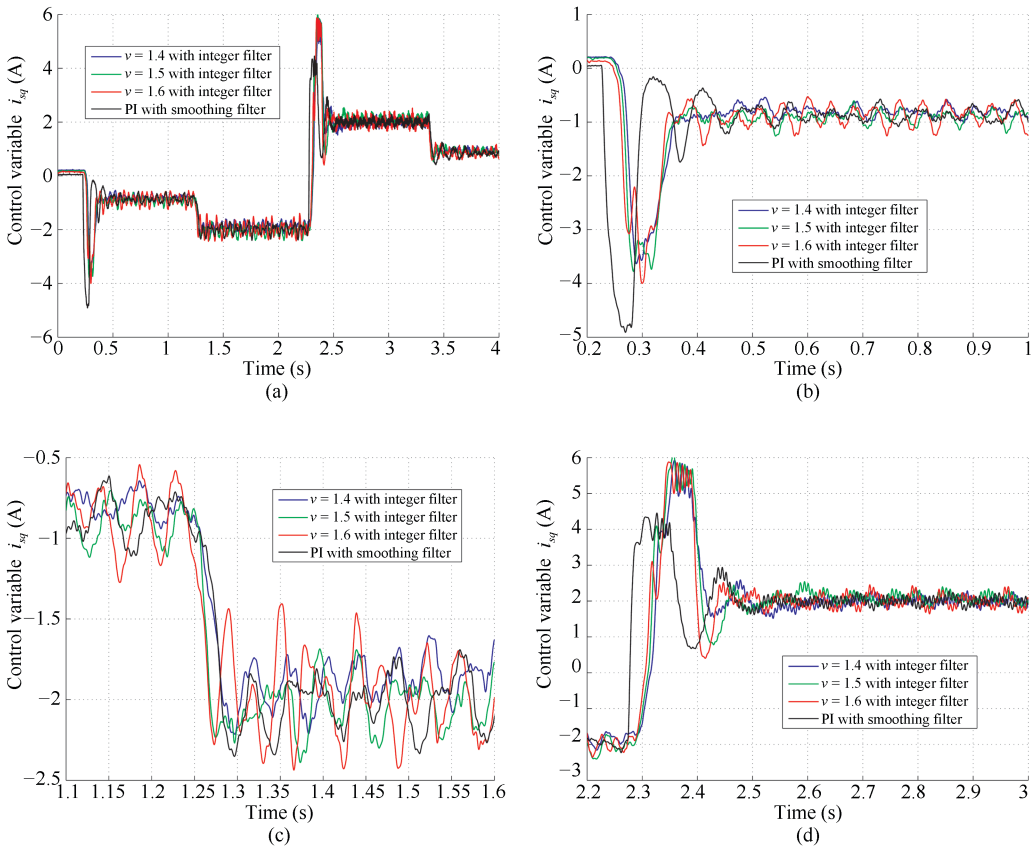

Fig. 9. Control variable when applying FOPI controllers and fractional filters. (a) General view. (b) Zoom in the no-load start period. (c) Zoom in the full load operational period. (d) Zoom in the period after full load speed reversal.

times, but they have much more oscillations (see Figs. 7(b)−7(c) and 8(b)−8(c)) and settle after slower transients.

In particular, using FOPI and integer filters reduces overshoots and undershoots with respect to using a standard PI with a smoothing pre-filter (see zoom in Fig. 7(b)), especially if ν is increased (the best response is with $\nu = 1.6$). The settling time is also reduced. Similar considerations hold true if fractional filters are employed (see zoom in Fig. 8(b)). The oscillations are much reduced with respect to the PI controller and a slightly faster response is obtained also with respect to integer filters.

Now, consider the ability to reject disturbances, then see the intermediate test period, which is better shown by Figs. 7(c) and 8(c). The zoom highlights that FOPI controllers achieve a better rejection of the applied load, especially if $\nu = 1.6$. Namely, the amplitude of the undershoot is much lower and the response settles in almost the same time as with a PI controller. To synthesize, the FOPI controller is beneficial for disturbance rejection which is very important in industrial applications.

Finally, Figs. 7(d) and 8(d) exhibit the last period in which the motion is reverted. Also in this condition, a FOPI controller with $\nu = 1.6$ reduces oscillations and obtains a fast settlement.

To complete the performance analysis, the control variable can be examined as well, for $\nu = 1.4, 1.5, 1.6$. Figs. 9(a)–9(d) show the results with fractional filters. An improvement is obtained with respect to the PI with a smoothing filter. Namely, see the reduction in oscillations and a faster response, which occurs especially after the reference input is applied (see Fig. 9(b)) and after the motion is reverted (see Fig. 9(d)). In any case, the speed response obtained by the PI with a smoothing filter is more rough, not completely clean and sensitive to disturbances (see Figs. 7 – 8).

VI. Conclusions

This paper proposes a new control scheme of DC-motor or PMSM drives, which are modeled as first-order systems plus a time delay. The scheme employs a fractional-order PI feedback controller and a set-point pre-filter, that can be of integer or fractional order. The feedback controller design is based on systematic closed-form expressions. The formulas allow easy and fast computation both of the controller parameters satisfying dynamic performance and robustness specifications (see (24) and (25) or (28)) and of the rational transfer function realization (see (29), (31), (32)). The pre-filter is designed by a dynamic inversion method that allows reducing overshoot to a large extent. The proposed scheme is compared with a classical one based on a standard PI controller combined with a smoothing pre-filter. The PI controller is tuned by the symmetrical optimum method, which is frequently employed in industrial cases. An extensive experimental (and simulation) analysis has shown the superior performance of the novel scheme and its potential impact.

References

[1] M. D. Ortigueira, *Fractional Calculus for Scientists and Engineers*. Dordrecht, The Netherlands: Springer, 2011.

[2] J. Sabatier, O. P. Agrawal, and J. A. Tenreiro Machado, *Advances in Fractional Calculus: Theoretical Developments and Applications in Physics and Engineering*. Netherlands: Springer, 2007.

[3] R. Caponetto, G. Dongola, L. Fortuna, and I. Petráš, *Fractional Order Systems: Modeling and Control Applications*. Singapore: World Scientific, 2010.

[4] C. A. Monje, Y. Q. Chen, B. M. Vinagre, D. Y. Xue, and V. Feliu, *Fractional-Order Systems and Controls: Fundamentals and Applications*. London, UK: Springer-Verlag, 2010.

[5] P. Arena, R. Caponetto, L. Fortuna, and D. Porto, *Nonlinear Noninteger Order Circuits and Systems: An Introduction*. Singapore: World Scientific, 2000.

[6] M. D. Ortigueira and J. A. Tenreiro Machado, "Special issue editorial: Fractional signal processing and applications," *Signal Process.*, vol. 83, no. 11, pp. 2285−2286, Nov. 2003.

[7] Y. Q. Chen and B. M. Vinagre, "A new IIR-type digital fractional order differentiator," *Signal Process.*, vol. 83, no. 11, pp. 2359−2365, Nov. 2003.

[8] R. R. Nigmatullin, C. Ceglie, G. Maione, and D. Striccoli, "Reduced fractional modeling of 3D video streams: The FERMA approach," *Nonlinear Dyn.*, vol. 80, no. 4, pp. 1869−1882, Jun. 2015.

[9] N. Engheta, "On the role of fractional calculus in electromagnetic theory," *IEEE Antennas Propag. Mag.*, vol. 39, no. 4, pp. 35−46, Aug. 1997.

[10] P. Bia, D. Caratelli, L. Mescia, R. Cicchetti, G. Maione, and F. Prudenzano, "A novel FDTD formulation based on fractional derivatives for dispersive Havriliak-Negami media," *Signal Process.*, vol. 107, pp. 312−318, Feb. 2015.

[11] A. Oustaloup, *La Commande CRONE. Commande Robuste d'Ordre Non Entiér*. Paris: Editions Hermés, 1991.

[12] I. Podlubny, "Fractional-order systems and $PI^{\lambda}D^{\mu}$-controllers," *IEEE Trans. Autom. Control*, vol. 44, no. 1, pp. 208−214, Jan. 1999.

[13] A. Oustaloup, F. Levron, B. Mathieu, and F. M. Nanot, "Frequency-band complex noninteger differentiator: characterization and synthesis," *IEEE Trans. Circuits Syst. I, Fundam. Theory Appl.*, vol. 47, no. 1, pp. 25−39, Jan. 2000.

[14] K. J. Åström and T. Hägglund, *PID Controllers: Theory, Design, and Tuning*, 2nd ed. Research Triangle Park, NC: Instrument Society of America, 1995.

[15] Y. Q. Chen, "Ubiquitous fractional order controls?," in *Proc. 2nd IFAC Symp. Fractional Derivatives and Applications FDA'06*, Porto, Portugal, 2006, pp. 168−173.

[16] H. W. Bode, *Network Analysis and Feedback Amplifier Design*. New York: Van Nostrand, 1945.

[17] C. A. Monje, B. M. Vinagre, V. Feliu, and Y. Q. Chen, "Tuning and auto-tuning of fractional order controllers for industry applications," *Control Eng. Pract.*, vol. 16, no. 7, pp. 798−812, Jul. 2008.

[18] R. S. Barbosa, J. A. Tenreiro Machado, and I. M. Ferreira, "Tuning of PID controllers based on Bode's ideal transfer function," *Nonlinear Dyn.*, vol. 38, no. 1−4, pp. 305−321, Dec. 2004.

[19] H. S. Li, Y. Luo, and Y. Q. Chen, "A fractional order proportional and derivative (FOPD) motion controller: Tuning rule and experiments," *IEEE Trans. Control Syst. Technol.*, vol. 18, no. 2, pp. 516−520, Mar. 2010.

[20] F. Padula, R. Vilanova, and A. Visioli, "H_{∞} optimization-based fractional-order PID controllers design," *Int. J. Robust Nonlinear Control*, vol. 24, no. 17, pp. 3009−3026, Nov. 2014.

[21] S. Stasi, L. Salvatore, and F. Cupertino, "Speed sensorless control of PMSM via linear Kalman filtering," *J. Electr. Eng.*, vol. 6, no. 4, pp. 1−8, 2006.

[22] R. C. Oldenbourg and H. Sartorius, "A uniform approach to the optimum adjustments of control loops," in *Frequency Response*, R. Oldenburger, Ed. New York: The Macmillan Co., 1956.

[23] C. Kessler, "Das symmetrische optimum," *Regelungstechnik*, vol. 6, pp. 395−400, 432−436, 1958.

[24] A. A. Voda and I. D. Landau, "A method for the auto-calibration of PID controllers," *Automatica*, vol. 31, no. 1, pp. 41−53, Jan. 1995.

[25] P. Lino and G. Maione, "Loop-shaping and easy tuning of fractional-order proportional integral controllers for position servo systems," *Asian J. Control*, vol. 15, no. 3, pp. 796−805, May 2013.

[26] R. E. Kalman, "When is a linear control system optimal?," *Trans. ASME Ser. D: J. Basic Eng.*, vol. 86, no. 1, pp. 51−60, Mar. 1964.

[27] J. M. Maciejowski, *Multivariable Feedback Design*. Wokingham, UK: Addison-Wesley, 1989.

[28] B. M. Vinagre, I. Podlubny, A. Hernández, and V. Feliu, "Some approximations of fractional order operators used in control theory and applications," *Fract. Calc. Appl. Anal.*, vol. 3, no. 3, pp. 231−248, 2000.

[29] Y. Q. Chen, B. M. Vinagre, and I. Podlubny, "Continued fraction expansion approaches to discretizing fractional order derivatives-an expository review," *Nonlinear Dyn.*, vol. 38, no. 1−4, pp. 155−170, Dec. 2004.

[30] R. S. Barbosa, J. A. Tenreiro Machado, and M. F. Silva, "Time domain design of fractional differintegrators using least-squares," *Signal Process.*, vol. 86 no. 10, pp. 2567−2581, Oct. 2006.

[31] G. Maione, "Continued fractions approximation of the impulse response of fractional-order dynamic systems," *IET Control Theory Appl.*, vol. 2, no. 7, pp. 564−572, Jul. 2008.

[32] G. Maione, "Conditions for a class of rational approximants of fractional differentiators/integrators to enjoy the interlacing property," in *Proc. of the 18th IFAC World Congr.*, S. Bittanti, A. Cenedese, S. Zampieri, Eds. Milan, Italy: IFAC, 2011, pp. 13984−13989.

[33] G. Maione, "Closed-form rational approximations of fractional, analog and digital differentiators/integrators," *IEEE J. Emerg. Sel. Topics Circuits Syst.*, vol. 3, no. 3, pp. 322−329, Sep. 2013.

[34] G. Maione, "Correction to "Closed-form rational approximations of fractional, analog and digital differentiators/integrators," *IEEE J. Emerg. Sel. Topics Circuits Syst.*, vol. 3, no. 4, pp. 654, Dec. 2013.

[35] G. Maione, "A rational discrete approximation to the operator $s^{0.5}$," *IEEE Signal Process. Lett.*, vol. 13, no. 3, pp. 141−144, Mar. 2006.

[36] G. Maione, "Concerning continued fractions representation of noninteger order digital differentiators," *IEEE Signal Process. Lett.*, vol. 13, no. 12, pp. 725−728, Dec. 2006.

[37] G. Maione, "High-speed digital realizations of fractional operators in the delta domain," *IEEE Trans. Autom. Control*, vol. 56, no. 3, pp. 697−702, Mar. 2011.

[38] G. Maione, "On the Laguerre rational approximation to fractional discrete derivative and integral operators," *IEEE Trans. Autom. Control*, vol. 58, no. 6, pp. 1579−1585, Jun. 2013.

[39] F. Padula and A. Visioli, "Inversion-based set-point filter design for fractional control systems," in *Proc. 2014 Int. Conf. on Fractional Differentiation and Its Applications*, Catania, Italy: IEEE, 2014, pp. 1−6.

[40] F. Padula and A. Visioli, "Inversion-based feedforward and reference signal design for fractional constrained control systems," *Automatica*, vol. 50, no. 8, pp. 2169−2178, Aug. 2014.

[41] A. Piazzi and A. Visioli, "Optimal noncausal set-point regulation of scalar systems," *Automatica*, vol. 37, no. 1, pp. 121−127, Jan. 2001.

Paolo Lino received the Laurea degree in electrical engineering from Politecnico di Bari, Italy, in 2000 and the Ph.D. degree in electronics and automation from the University of Catania, Italy, in 2004. In 2003 he has been a visiting researcher at the University of New Mexico, Albuquerque, NM, USA. Currently he is an assistant professor in automatic control at Politecnico di Bari. His main research interests are in intelligent control, predictive control and modeling and control of electro-mechanical and automotive systems. He is co-author of more than 60 peer reviewed papers in journals, book chapters, and conference proceedings. Dr. Lino is member of IEEE and IEEE Control Systems Society.

Guido Maione received the Laurea degree with honors in electronic engineering in 1992 and the Ph.D. degree in electrical engineering in 1997, both from Politecnico di Bari. In 1996 he joined the University of Lecce, Italy, where he was assistant professor in automatic control. In 2002 he moved to Politecnico di Bari. He visited the Rensselaer Polytechnic Institute of Troy, NY, USA, in 1997 and 1998, and the Queen's University of Belfast (UK) in 2007, 2009, and 2013. His research interests include fractional-order systems and controllers, automotive systems, discrete event systems, multi-agent systems, Petri nets and digraph models. He is the author or co-author of more than 120 peer reviewed papers in journals, book chapters and conference proceedings. Dr. Maione is senior member of IEEE, IEEE Control Systems Society, and he is an IFAC affiliate. In 1996 he founded the IEEE Student Branch at Politecnico di Bari and served as first ad interim president. Corresponding author of this paper.

Silvio Stasi received the M.Sc. degree in electrical engineering from the University of Bari, Italy, in 1989, and the Ph.D. degree in electrical engineering from Politecnico di Bari, in 1993. From 1990 to 1993, he was with the Electric Drives and Machines Group, Politecnico di Bari, where he carried out research on control and state and parameter estimation of electrical drives and, since November 2002, he has been an associate professor of electrical machines and drives in the Department of Electrical and Information Engineering. His research interests include control of electric drives, fuzzy logic, neural networks, power electronics, and motor parameter estimation.

Fabrizio Padula received the M.Sc. degree in industrial automation engineering in 2009 and the Ph.D. degree in computer science and automatic control in 2013, both form the University of Brescia. Currently, he is research fellow at the Department of Mathematics and Statistics of the Faculty of Science and Engineering at Curtin University, Perth, Australia. His research activity deals with fractional control, inversion-based control and tracking control. He is also interested in robotics and mechatronics.

Antonio Visioli received the Laurea degree in electronic engineering from the University of Parma in 1995 and the Ph.D. degree in applied mechanics from the University of Brescia in 1999. Currently he holds a professor position in automatic control at the Department of Mechanical and Industrial Engineering of the University of Brescia. He is a senior member of IEEE and a member of the TC on Education of IFAC, of the IEEE Control Systems Society TC on Control Education and of the IEEE Industrial Electronics Society TC on Factory Automation Subcommittees on Event-Based Control & Signal and on Industrial Automated Systems and Control, and of the National Board of Anipla (Italian Association for Automation). His research interests include industrial robot control and trajectory planning, dynamic inversion based control, industrial control, and fractional control. He is the author or co-author or editor of four international books, one textbook and more than 200 papers in international journals and conference proceedings.